# Reduction of force exciting influences to decrease radiation of acoustic noise in synchronous machines

Stephan Schulte and Kay Hameyer
*Institute of Electrical Machines, RWTH Aachen University, Aachen, Germany*

## Abstract

**Purpose** – The paper aims to provide an approach to actively decrease the radiation of acoustic noise in synchronous machines.

**Design/methodology/approach** – Splitting regular three-phase windings of synchronous machines into two independent three-phase systems allows for an active influence of the current waveform if both winding systems are mutually displaced against each other. The harmonics content of each phase-current varies due to the mutual inductive coupling with participating currents of both systems. Therefore, the ensuing force-density distribution on the stator teeth varies accordingly. Resulting structure dynamics and furthermore the radiation of relevant harmonics of the acoustic noise are based on the mechanical excitation of considered force-density distributions.

**Findings** – Configurations of mutual displacement of phase windings of both winding systems with significant decrease of mechanical deformation and emitted acoustic noise are found. Simulation methods to entirely describe and prove the behavior described are developed.

**Research limitations/implications** – The proposed approach is developed for a particular synchronous machine. Other machine types are conceivable for analysis in the same manner. Tools need to be adapted. Universal and reliable statements regarding acoustic behavior depend on the mechanical restraint of the machine and may therefore vary.

**Practical implications** – Active force-density distribution is used for the noise reduction of alternators in vehicle applications. Additionally, wind-power generators are considered for the application of split stator winding systems to actively counteract inhomogeneous force distributions on the rotor, evoked by stalling of the propeller blades during pole passing.

**Originality/value** – Active force-density modification by stator winding modifications allows for the decrease of noise radiation of electrical machines with rotating-field windings. Innovative simulation methods developed may now replace prototyping partially.

**Keywords** Noise control, Electric machines

**Paper type** Research paper

## 1. Design approach

Commonly used CPAs consist of a claw-pole rotor and a stator of stacked laminations, carrying a regular three-phase winding. A symmetry cut out of the rotor and stator arrangement is shown in Figure 1. Stator coils are modeled with simplified end windings, sufficient for analysis steps processed.

The accordant stator winding arrangement is shown in Figure 2, based on the phasor diagram as of Figure 3. A regular three-phase winding ($m = 3$) using phases U, V and W with a stiff phase displacement $\alpha_m = \pm 120°$ between each other is given.

COMPEL: The International Journal for Computation and Mathematics in Electrical and Electronic Engineering
Vol. 26 No. 4, 2007
pp. 1017-1027

0332-1649
DOI 10.1108/03321640710756348

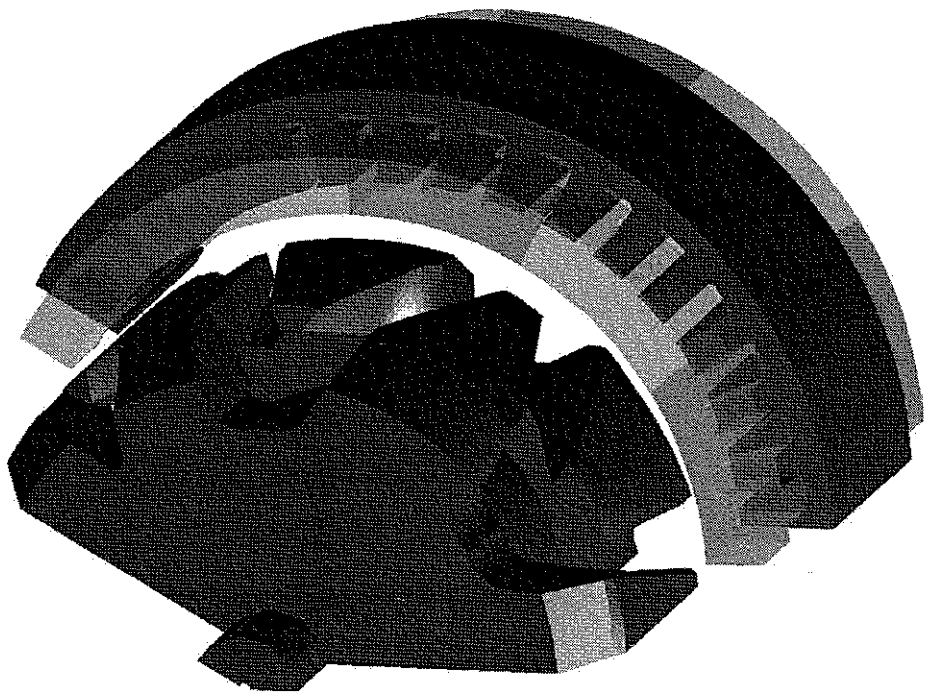

**Figure 1.**
Rotor and stator (with windings) of a CPA

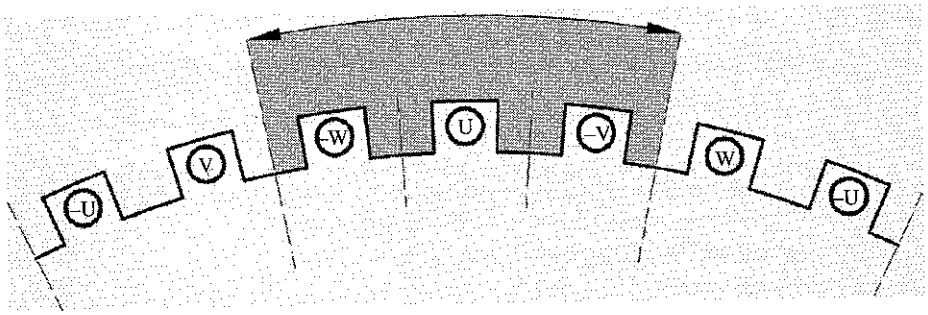


**Figure 2.**
Windings in stator slots ($m = 3$)

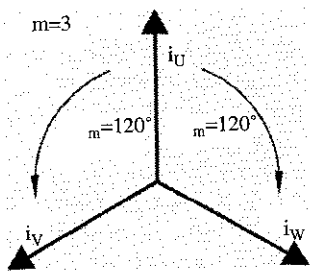


**Figure 3.**
Current-phasor diagram ($m = 3$)

The correspondence of the air-gap field and the stator magnetomotive force (mmf) excite force stress on the stator teeth of electrical machines. These are leading to deformation and furthermore to radiation of acoustic noise.

The utilization of winding systems with more than three phases reduces the currents density and therefore the mmf per phase as a matter of fact. Choosing a six-phase winding (Schulte and Henneberger, 2004; Schulte *et al.*, 2004a, b) allows for the operation as two independent three-phase systems with arbitrary connection – either systems in star or delta connection or one different than another. Examples are shown in Figure 4 for both systems arranged in flying star (left) as well as in star connection with common ground (right).

A decreased current stress on rectifier diodes and windings allows for a reduced diameter of the winding wires.

Therefore, any stator slot carries windings of both independent three-phase systems (at the same number of turns as previously implemented for the three-phase configuration).

The accordant two-layer arrangement of both winding systems is shown in Figure 5, the applicable current-phasor diagram is shown in Figure 6.

If free to displace one of the three-phase windings against the other, the phase shift of the currents of both windings systems varies due to the effect of mutual induction of all participating phase currents as well as the excitation current.

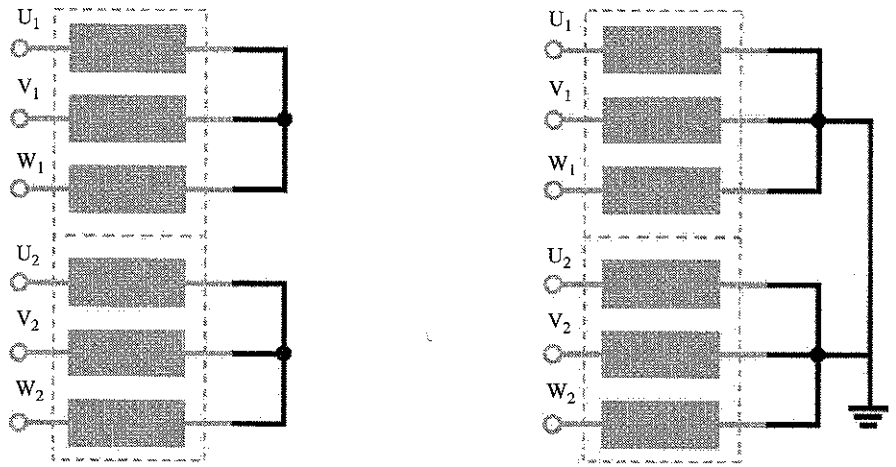


**Figure 4.**
Flying star and star connection of winding systems ($m = 6$)

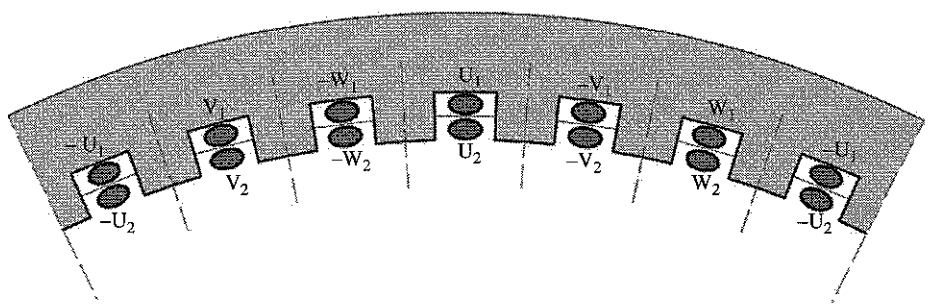


**Figure 5.**
Windings in stator slots ($m = 6$)

The equations of two exemplarily selected phase currents (one of each winding system) read as follows:

$$i_{U1} = \frac{\psi_{U1}}{L_{U1}} - i_{V1}\frac{L_{U1V1}}{L_{U1}} - i_{W1}\frac{L_{U1W1}}{L_{U1}} - i_{U2}\frac{L_{U1U2}}{L_{U1}}, \\ - i_{V2}\cdot\frac{L_{U1V2}}{L_{U1}} - i_{W2}\cdot\frac{L_{U1W2}}{L_{U1}} - i_F\cdot\frac{L_{U1F}}{L_{U1}} \tag{1}$$

$$i_{U2} = \frac{\psi_{U2}}{L_{U2}} - i_{U1}\frac{L_{U1U2}}{L_{U2}} - i_{V1}\frac{L_{V1U2}}{L_{U2}} - i_{W1}\frac{L_{W1U2}}{L_{U2}}, \\ - i_{V2}\cdot\frac{L_{U2V2}}{L_{U2}} - i_{W2}\cdot\frac{L_{U2W2}}{L_{U2}} - i_F\cdot\frac{L_{U2F}}{L_{U2}}. \tag{2}$$

Initially displacement steps $\alpha_V$ of multiples of an integer slot pitch appear most reasonable. Figure 7 shows a stator-winding configuration with one slot displacement. Contents of stator-slots are simplified shown as lumped windings.

The applicable current-phasor diagram for the configuration shown in Figure 7 appears as of Figure 8.

Symmetry of the electrical behavior is reached after two slots displacement, merely stating a low number of configuration varieties. That leads to feasible displacement angles:

$$\alpha_V = k\cdot 60°(k = 0\ldots 2). \tag{3}$$

In fact, stator slots contain a number of $w$ windings. This number of windings may be distributed onto more than one slot, leading to a distributed arrangement of accordant phase currents and a slurred mmf distribution. An assumed number of $w = 8$ windings

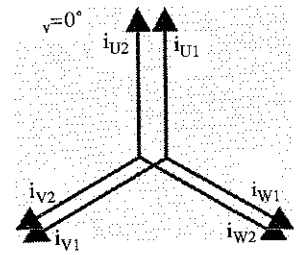


**Figure 6.**
Current-phasor diagram ($m = 6$)

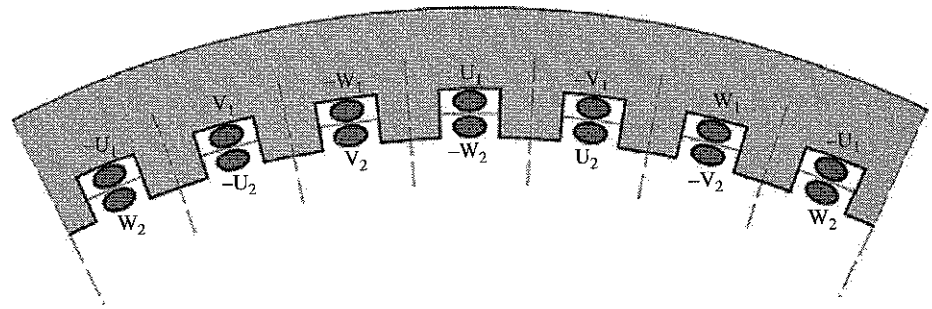


**Figure 7.**
Slot-wise displacement ($m = 6$) – one slot shifted

allows for altogether 16 wire-wise displacement steps, resulting from a wire-wise shift along two stator slots as mentioned in equation (3):

$$\alpha_V = \frac{k}{8}60°(k = 0...16). \quad (4)$$

Figure 9 shows a wire-wise displacement of two wires ($k = 2$), shifted to adjacent stator slots each.

## 2. Computation approach

### *2.1 Macrostructural analysis*

A simulation model of the alternator, implemented in VHDL-AMS (IEEE, 1993) for hardware description, is used to determine all phase currents of both winding systems accordant to the mutual displacement of their winding system. The machine model contains a set of differential equations for phase currents equations (1) and (2), flux linkages, mutual inductances, and torque as well as motion equations. This machine model is embedded into a simplified vehicle power supply system consisting of excitation circuit, 12-pulse rectifier bridge and electrical load. The entire environment, called system model, is shown in Figure 10.

Figure 11 shows phase currents of system No. 1 (index 1) and accordant currents of system No. 2 (index 2) for two selected displacement angles $\Delta\alpha_V$ to emerge from system simulations of a specified operational point (→ details and particular values not presented due to nondisclosure obligation).

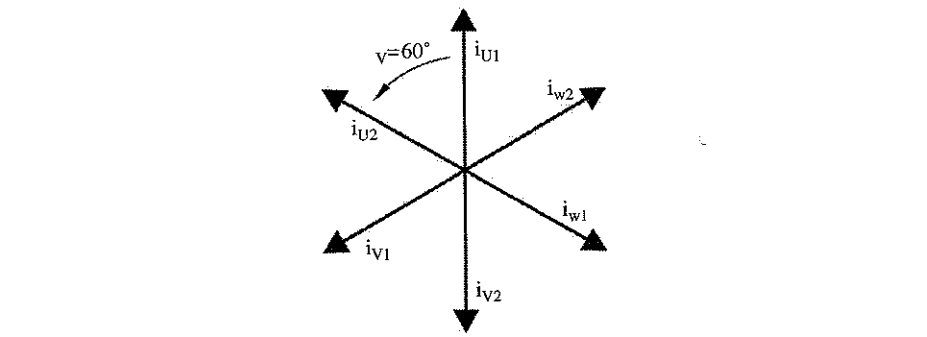


**Figure 8.**
Current-phasor diagram due to winding arrangement as of Figure 7

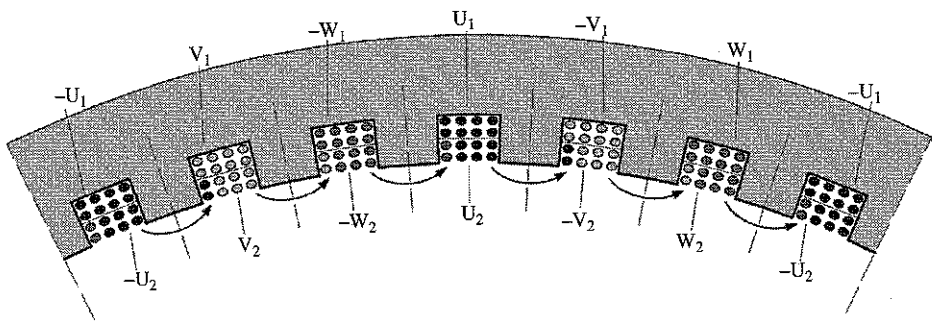


**Figure 9.**
Wire-wise displacement ($m = 6$) – two wires shifted

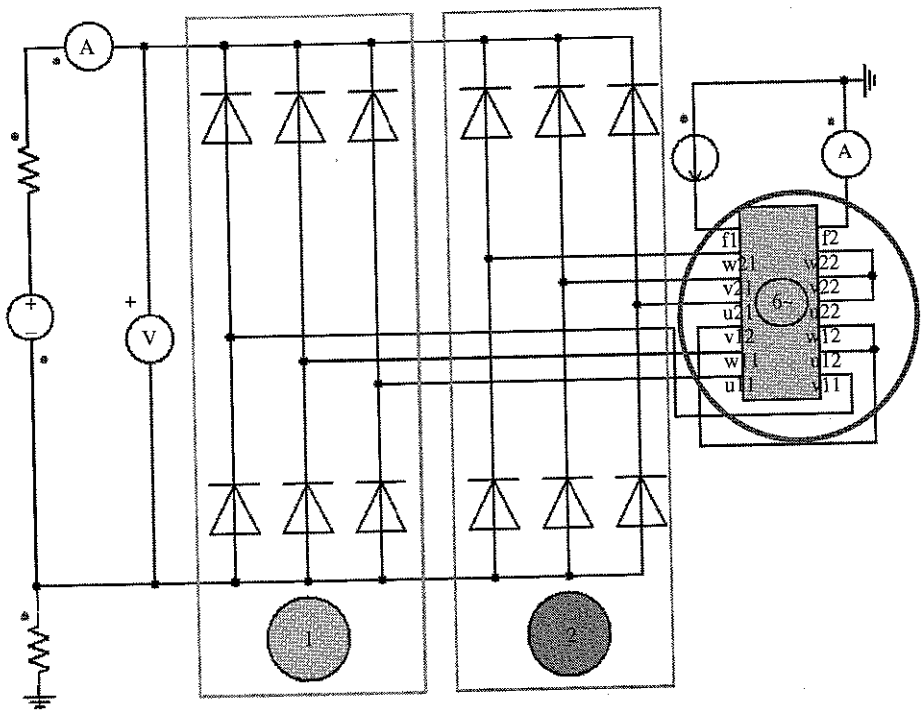


**Figure 10.**
System simulation environment with machine model (circled)

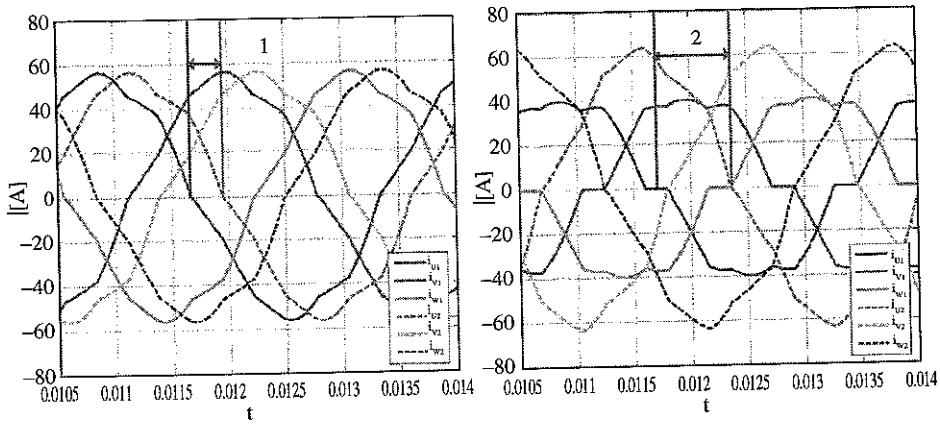


**Figure 11.**
Phase current mutation due to winding displacement $\Delta\alpha_V$

The mutation of the current shape, dependent on the winding displacement, affects amplitude, phase angle and harmonic content of the currents equations (1) and (2). Figure 12 shows differences in the harmonic current components of the selected phase current $i_{U1}$ (belonging to system No.1), whereas Figure 13 shows the harmonics content of the torque $M_{el}$ exerted on the shaft.

Thus, since applicable phase currents and related flux linkages state the torque creating and force exciting components (the latter applied to stator teeth), the harmonic

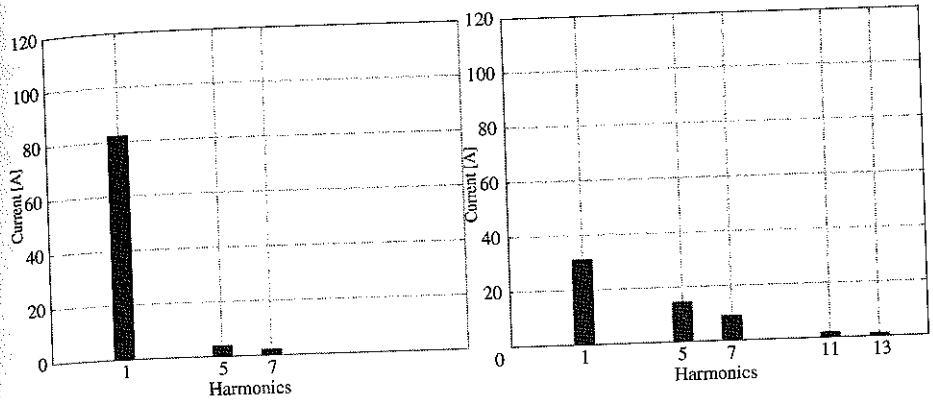


**Figure 12.**
Current harmonics of selected phase current of system No.1

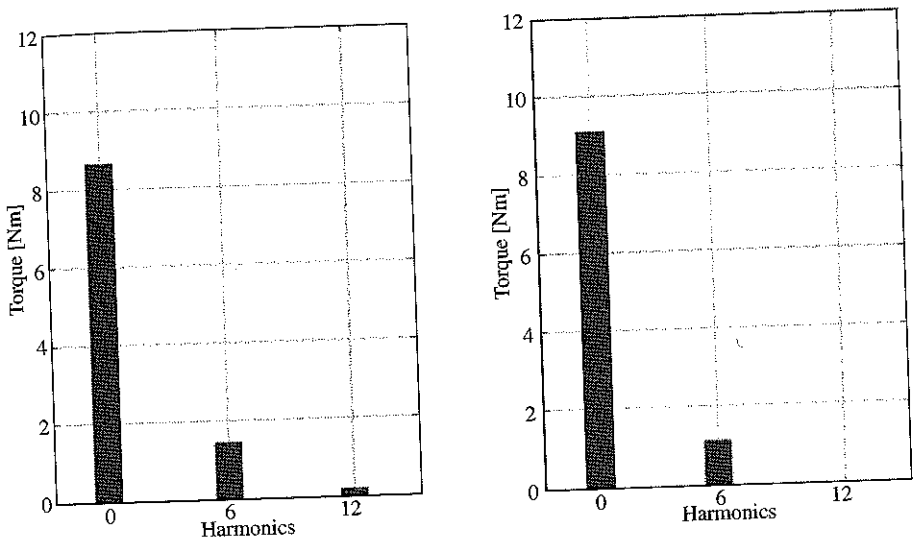


**Figure 13.**
Torque harmonics for selected winding configurations

content of stator teeth forces can be influenced. Therefore, the mutual displacement of the two 3-phase winding systems provides a means to reduce significant force excitation leading to lower radiation of acoustic noise, as presented in the following.

*2.2 Microstructural analysis*

Phase currents thus determined characterize the electrical excitation to be injected into continuative electromagnetical FE simulations. The flux density distribution emerging from the electromagnetical FE simulations is used for the computation of the force stress on the stator teeth.

A subsequently processed Fourier analysis is utilized for detecting the harmonics content of the force density distribution. This is followed by a frequency-selective appliance of the force stress on the mechanical FE model of the alternator, stating the basis for the computation of the structure-dynamic deformation.

Figure 14 shows the deformation of the mechanical machine model analyzed for a specified operational point – including stator iron, winding and housing (scale factor of the deformation: 1:50.000 – used for visualization purposes).

The evaluation of graphical results turns out to be non-reasonable due to comparability. Therefore, the determination of the body sound is chosen as the most reasonable option, since appearing as quantitative means. Other than for the common determination of the body sound of single nodes according to their displacement, an integral measure is introduced to cover the entire machine. The radiation of body sound $L_{BS}(\Omega)$ computes to:

$$L_{BS}(\Omega) = 10 \log \left( \frac{\sum_{p=1}^{N} \int_{Sp} |\underline{v}_p \cdot \underline{n}^p|^2 \mathrm{d}S}{S_0 \cdot h_{U_0}^2} \right) \mathrm{d}B. \tag{5}$$

$S$ means the surface, $n^P$ the normal vector of the $p$th element. The variable $\underline{v}_p$ represents the velocity of the accordant node, adjusting independently from the force stress. $S_0 \cdot h_{U_0}^2$ is introduced as reference value for normalization (van Riesen and Henneberger, 2002). Saturation effects, simulated temperature feedback as well as losses, such as eddy current or ohmic losses are implemented and regarded using a bi-directional coupling between both simulation approaches presented. At first the microstructural computation allows for considering the state of saturation and therefore defines inductances to occur to due the applicable excitational state. Secondly, inductances thus determined are utilized for the simulation of resulting phase currents within the macrostructural system simulation approach. These currents define the excitation to be used for the microstructural FE simulation again.

The interconnection of phase windings of each system remains unconsidered in this paper. However, the interconnection chosen (e.g. star or delta) can easily be varied on the schematic within the macrostructural system simulation.

## 3. Results

As of (Xu and Ye, 1995) the fifth and even more the six harmonic of the body sound appear dominantly for the radiation of acoustic noise so that focus is put on the reduction of these harmonics.

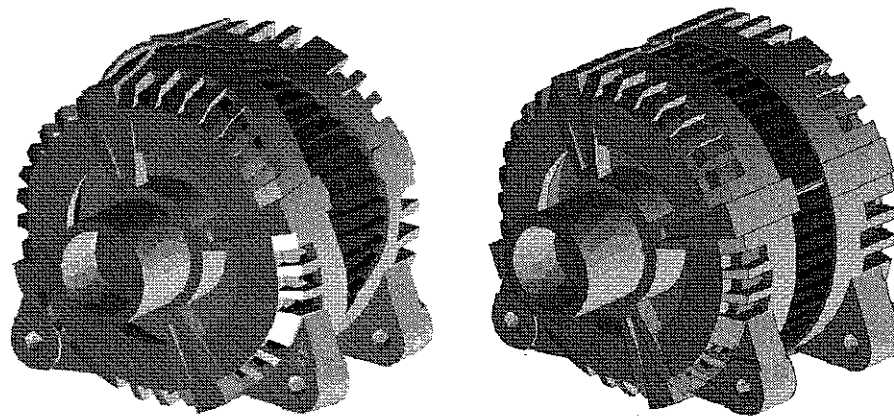

**Figure 14.**
Deformed/non-deformed generator due to force stress

Figure 15 shows a configuration to be found with a significant reduction almost 10 dB of the sixth harmonic of the body sound as a result of a reasonable choice of the winding displacement (left) – compared to the worst case configuration (right).

The reduction of the sixth harmonic of the body sound comes along with an unwanted reduction of the output power for the chosen winding configuration.

In general, the output power of alternators in vehicle applications computes from the output current (that is the DC-link current in the rectifier bridge) and the DC-link voltage (equal to the battery voltage).

The DC-link current, resulting from adding all six currents portions of the participating stator phases is shown in Figure 16. Different shapes of the DC-link current and therefore a varied composition of harmonics contained are studied – not providing information regarding the output power.

Therefore, a depiction of the root-mean square (RMS) values of the DC-link currents is required. See Figure 17 for three samples, showing a selection of prominent winding configurations (best and worse case concerning output power as well as the chosen variant regarding lowest radiation of body sound sixth harmonic).

Simulations are utilized as an alternative to cost and time expensive prototype manufacturing.

The machine concept presented, characterized by a large number of winding configurations states a typical application for simulations replacing prototype manufacturing at early design stages, since simulations allow for easy parameter variation. At the current design stage there is no existing prototype available for measurements taken as a reference. Although the computation concept presented provides reliable results since utilized tools are verified in previous applications (van Riesen and Henneberger, 2002).

## 4. Conclusions

Varying the mutual displacement between two independent three-phase systems placed in a stator of a regular claw pole alternator (forming a six-phase system) allows for influencing amplitude and shape and therefore, the harmonic content of force exciting parameters such as current and flux linkage. A particular displacement angle is found featuring a minimum of body sound generation, still stating an

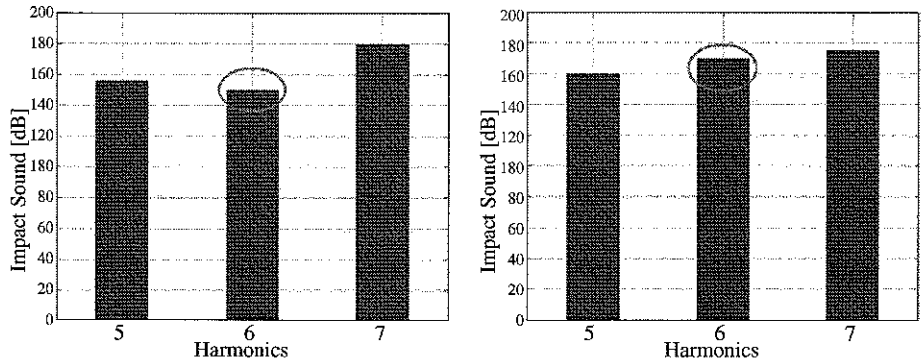


**Notes:** Best: left, worst: right

**Figure 15.**
Fifth to seventh harmonics of body sound based on accordant winding configurations

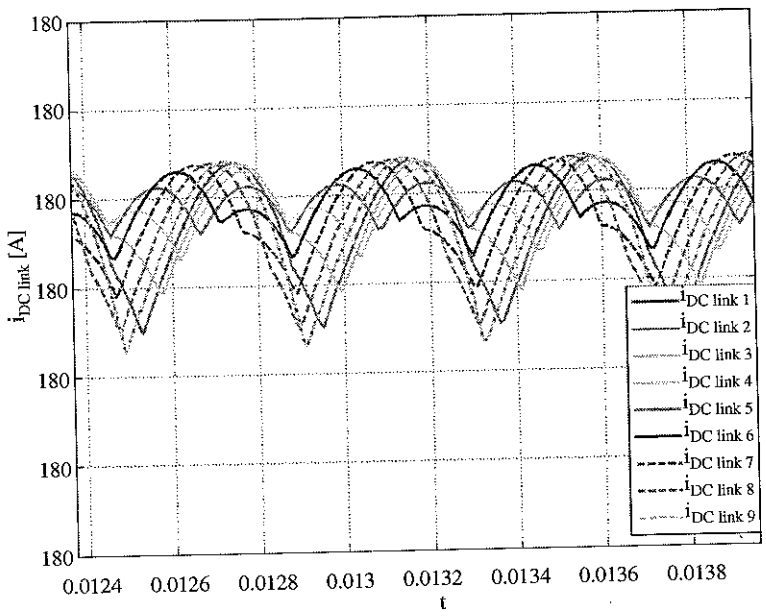


**Figure 16.**
DC-link currents for different winding configurations

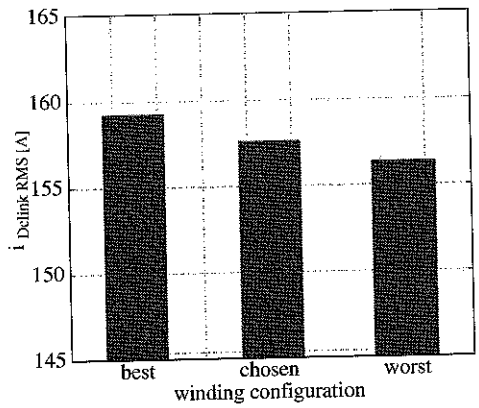


**Figure 17.**
DC-link currents (RMS) for selected winding configurations

acceptable forfeit of the output power coming along herein. The simulation approach utilized turned out successful.

## References

IEEE (1993), "VHDL-AMS: Very High Speed Hardware Description Language – Analog and Mixed Signals", *IEEE Standard 1076.1-1993*.

Schulte, S. and Henneberger, G. (2004), "Current-waveform analysis of 6-phase claw-pole alternators using VHDL-AMS implementation in Simplorer", *Proceedings ICEM 2004, Cracow (Poland)*.

Schulte, S., Kaehler, C., Schlensok, C. and Henneberger, G. (2004a), "Combined analytical and numerical computation approach for design and optimization of 6-phase claw-pole alternators", *IEE Journal on Proc.-Sci. Meas. Technol.*, Vol. 151 No. 6.

Schulte, S., Kaehler, C., Schlensok, C. and Henneberger, G. (2004b), "Stator optimization of 6-phase claw-pole alternators using asymmetric winding arrangements", *COMPEL*, Vol. 23 No. 3.

van Riesen, D. and Henneberger, G. (2002), "Electrical, mechanical and acoustic analysis of an induction furnace using finite element methods", paper presented at the 3rd International Seminar on Vibration and Acoustic Noise in Electric Machinery - VANEM, S. 41-45. Lodz (Poland).

Xu, L. and Ye, L. (1995), "Analysis of a novel stator winding structure minimising harmonic current and torque ripple for dual sixstep converter-fed high power AC machines", *IEEE Trans. Industry Appl.*, Vol. 31 No. 1.

## Further reading

Lyra, R. and Lipo, T.A. (2002), "Torque density improvement in a six-phase induction motor with third harmonic current injection", *IEEE Trans. On Industry Applications*, Vol. 38 No. 5, pp. 1351-60.

van Riesen, D., Monzel, C., Kaehler, C., Schlensok, C. and Henneberger, G. (2004), "iMOOSE - an open-source environment for finite-element calculations", *IEEE Trans. on Magnetics*, Vol. Bd. 40, Nr. 2 S, pp. 1390-3.

## About the authors

Stephan Schulte, born on January 28, 1976, studied Electrical Engineering at RWTH Aachen University, graduated with Diploma in 2002, received PhD in 2006, currently working with the Institute of Electrical Machines (IEM) of RWTH Aachen University.

Kay Hameyer received a PhD from the University of Technology Berlin, Germany, 1992. From 1986 to 1988 he worked with the Robert Bosch Gmbh in Stuttgart, Germany, as a Design Engineer for permanent magnet servo-motors. In 1988 he became a Member of the Staff at the University of Technology Berlin, Germany. He was next a Professor of Numerical Field Computation and Electrical Machines with the K.U. Leuven and a Senior Researcher with the FWO-V, Belgium, teaching CAD in electrical engineering and electrical machines. Since, 2004, he is Head of the Institute for Electrical Machines, with the RWTH Aachen University, Germany. His research interests are numerical field computation, the design of electrical machines, in particular permanent magnet excited machines, induction machines and numerical optimisation strategies. He is a member of the International Compumag Society and the IEEE. Kay Hameyer is the corresponding author and can be contacted at: Kay.Hameyer@iem.rwth-aachen.de